Talanta 94 (2012) 84–89

Contents lists available at SciVerse ScienceDirect

Talanta

journal homepage: www.elsevier.com/locate/talanta

Specific and targeted detection of viable *Escherichia coli O157:H7* using a sensitive and reusable impedance biosensor with dose and time response studies

Majed Dweik[a], R. Cody Stringer[a], Shibajyoti Ghosh Dastider[b], Yifan Wu[b], Mahmoud Almasri[b], Syed Barizuddin[a,*]

[a] *Co-operative Research and Life & Physical Sciences, Lincoln University, Jefferson City, MO 65101, USA*
[b] *University of Missouri, Department of Electrical and Computer Engineering, Columbia, MO 65211, USA*

ARTICLE INFO

Article history:
Received 12 December 2011
Received in revised form 20 February 2012
Accepted 22 February 2012
Available online 1 March 2012

Keywords:
Impedance sensing
E. coli O157:H7
Interdigitated microelectrodes (IDEA)

ABSTRACT

A gold interdigitated microelectrode (IME) impedance biosensor was fabricated for the detection of viable *Escherichia coli O157:H7*. This sensor was fabricated using lithography techniques. The surface of the electrode was immobilized with anti-*E. coli* IgG antibodies. This approach is different from other studies where the change in impedance is measured in terms of growth of bacteria on the electrode, rather then the antibody/antigen bonding. The impedance values were recorded for frequency ranges between 100 Hz and 10 MHz. The working range of the dose response for this device was found to be between 2.5×10^4 CFU ml^{-1} and 2.5×10^7 CFU ml^{-1}. The time response studies indicated that antibody/antigen binding is not a function of time, but can decrease if excess times are allowed for binding. It was observed that the impedance values for 60 min antibody/antigen binding were higher than the impedance values for 120 min binding time. The main advantages of the reported device are that, it provides for both qualitative and quantitative detection in 3 h while other impedance sensors reported earlier may take up to 24 h for detection. If enrichment steps are required then it may take 3–4 days to infer the results. This sensor can be used to detect different types of bacteria by immobilizing the antigen specific antibody. Most of the sensors are not reusable since they either use enzymes or enrichment steps for detection but this device can be reused, following a cleaning protocol which is easy to follow. Each device was used at least five times. The simplicity of this sensor and the ease of fabrication make this sensor a useful alternate to the microfluidics and enzyme based impedance sensors, which are relatively more difficult to fabricate, need programmable fluidic injection pumps to push the sample through the channel, suffer from limitation of coagulation and are difficult to clean.

1. Introduction

The recent outbreak of E.coli related infections and food recalls in Unites States, Europe and other parts of the world, again brings to the forefront the importance of fast and reliable detection of food borne pathogens at a very early stage to prevent ill effects on human health and mitigate the possibility of disruption in the food supply chain. The most common cause of the contamination in the food is due to the food borne pathogen *Escherichia coli* (*E. coli*) *O157:H7*. These are a large and diverse group of bacteria, some strains of which can cause diarrhea, while others can cause urinary tract infections, respiratory illness, pneumonia, and other illnesses [1]. *E. coli O157:H7* can easily contaminate food products and drinking water. Exposures that result in illness include consumption of contaminated food, unpasteurized milk and water that has not been disinfected, contact with cattle or contact with the feces of infected people. Some foods carry a high risk of *E. coli O157:H7* contamination that health officials recommend people avoid completely. These foods include unpasteurized milk, unpasteurized apple cider and soft cheeses made from raw milk. Other possibilities of becoming infected include swallowing lake water while swimming, touching animals in the zoo etc. [2]. The Center for Disease Control estimates that contaminated food causes approximately 1000 reported disease outbreaks and an estimated 48 million illnesses, 128,000 hospitalizations and 3000 deaths annually in the United States between [3]. The surveillance data reported includes trends between 1996 and 2010, which have remained consistent. Among all pathogens, *E. coli O157:H7* is a leading cause of food borne illness. The recent outbreaks of this type of bacteria has been detected in Lebanon Bologna, Hazelnut, cheese, beef, cookie dough, French spinach etc. between 2006 and 2011 [2,3]. *E. coli O157:H7* can cause huge health care costs and product recalls, hence the rapid and reliable detection of *E. coli O157:H7* has become very important.

The conventional methods for detecting *E. coli O157:H7* can require up to 60 h including the enrichment steps [4,5]. Extensive

* Corresponding author at: 334 Founders Hall, 816 Chestnut St., Jefferson City, MO 65101, USA. Tel.: +1 573 681 5137; fax: +1 573 681 5944.
E-mail address: barizuddins@lincolnu.edu (S. Barizuddin).

0039-9140/$ – see front matter © 2012 Elsevier B.V. All rights reserved.
doi:10.1016/j.talanta.2012.02.056

research is going onto develop new and rapid detection methods to replace traditional techniques which are labor intensive, time consuming and expensive. Quick and simple methods to detect this type of bacteria are essential to control the spread of pathogenic infestation in contaminated food and water, and to prevent infections and epidemics.

The current methods for detection of micro-organisms are dependent upon drawing a sample and then analyzing it. The different methodologies involved in the analysis include, but are not limited to: optical methods [6–8], electrochemical [9,10] and electronic methods [11–13]. Most of these methods are time consuming, tedious and put a limitation to their extensive and on-site use. Conventional microbiological methods for determining the cell counts of bacteria employ selective culture and biochemical and serological characterizations [14]. Although these methods achieve sensitive and selective bacterial detection, they typically require days to weeks to yield results. Many different technologies have shown potential for rapid and sensitive systems, but suffer from the limitations of low detection limit and differentiation between viable and non-viable cells. Amperometric biosensor [15–17], fiber-optic evanescent wave biosensor [18,19], electrochemistry [20–22], Immunomagnetic separation [6,23,11,24] are some examples.

The most commonly used method in detection of *E. coli* is based on the Polymerase chain reaction (PCR) [25–27]. This method is responsive to detection of low concentrations of bacteria and has been used in conjunction with other methods. The time required in using PCR method is shorter as compared with other traditional methods, but the method requires a complex set-up and trained personnel. Other methods developed for detection of *E. coli O157:H7* include a fluorescent bacteriophage assay capable of detecting 10^4 CFU ml^{-1}. Lower concentrations up to 10–10^2 CFU ml^{-1} *E. coli O157:H7* have also been detected after 10 h using enrichment step [28]. Immunomagnetic separation and solid-phase laser cytometry could detect 10 CFU g^{-1} within 5–7 h [29]. Enzyme-linked immunoassay (ELISA) has also been useful in the detection of *E. coli O157:H7*. Advantages of ELISA include high reproducibility and possibility for simultaneous quantification of a number of assays, but the enzymatic sensors are affected by atmospheric conditions such as temperature, humidity etc.

Other biosensors studied for detection of pathogenic bacteria include label-dependent immunosensors that use labeled secondary antibodies to translate the antibody/antigen bonding into a detectable signal. Label-free biosensors [30] and surface Plasmon resonance [31] have attractive advantages with respect to speed, cost, and simplicity of operation. Measuring change in the impedance to detect pathogens is another rapid and inexpensive alternate to label-free biosensors. In this method, microelectrodes are fabricated using standard lithographic processes [39]. Microelectrodes exhibit higher sensitivities than macroelectrodes and have semi-infinite linear diffusion profiles resulting in a greater depletion of reactants in contrast to the microelectrodes which have spherical diffusion profiles favoring a greater rate of reactant supply [32]. Other advantages of microelectrodes include low ohmic drop, faster reaction and increased signal-to-noise ratio. Interdigitated microelectrodes (IDEA) are frequently being used for measuring impedance, by capturing bacterial cells to the antibodies immobilized on the surface of electrodes [33]. Open IDEA chips were used in this study for the detection of *E. coli O157:H7* cells by immobilizing anti-*E. coli* antibodies on the surface of IDEA's for the capture of target bacteria.

Impedance measurement technique is employed for monitoring and detecting pathogens, antibiotics and analyzing food [34,35]. This indirect approach quantifies pathogens by measuring the change in the electrical impedance on the surface of the microelectrodes. Impedance measurement is commonly preferred over conductance measurement, which detects only the change in conductivity of the medium because of the bacterial growth. Impedance measurements account for both the double layer and dielectric capacitance. It has been estimated that a concentration of 10^3–10^7 CFU ml^{-1} of bacterial cells is required to produce a detectable change in the impedance signal [36,37].

The capability of IDEA's can be further enhanced by incorporating microfluidics. The advantages of these are high detection sensitivity, small volume handling, and low contamination during bacterial growth and rapid detection of a small number of cells. The surface to volume ratio increases in the microfluidic flow with embedded IDEA, and the distance that conductive ions must diffuse to reach the sensor surface decreases, thus resulting in faster reaction kinetics [37]. Current impedance sensing techniques that use microfluidics are based on the complex multi-step design of a flow cell with an embedded IDEA which has limited applications due to clogging and difficulty cleaning [30,38].

2. Experimental

2.1. Interdigitated microelectrode fabrication

In this study an impedance biosensor was fabricated on a glass substrate using conventional surface micromachining and photolithography processes [40]. A layer of chromium (Cr) and gold (Au) with a thickness of 50 nm and 200 nm, respectively, was used as the electrode material. These layers were deposited using RF magnetron sputtering system. The Cr serves as an adhesion layer for Au. The interdigitated electrode array consists of 100 finger pairs with a length, width, and spacing between fingers of 1.5 mm and 15 μm, and 10 μm, respectively. They were patterned by etching Au and Cr as shown in the Fig. 1. A Polydimethylsiloxane (PDMS) slabs was made and cured to serve as a reservoir for holding the media containing antibody over the interdigitated electrode array. The PDMS slab was bonded to the glass substrate using oxygen plasma treatment that changes its surface to hydrophilic and hence form excellent bond with the glass substrate. Au electrodes are perfectly polarized, hard to oxidize and do not react with the medium. They also exhibit strong capacitive effect. Cr layer was used as an

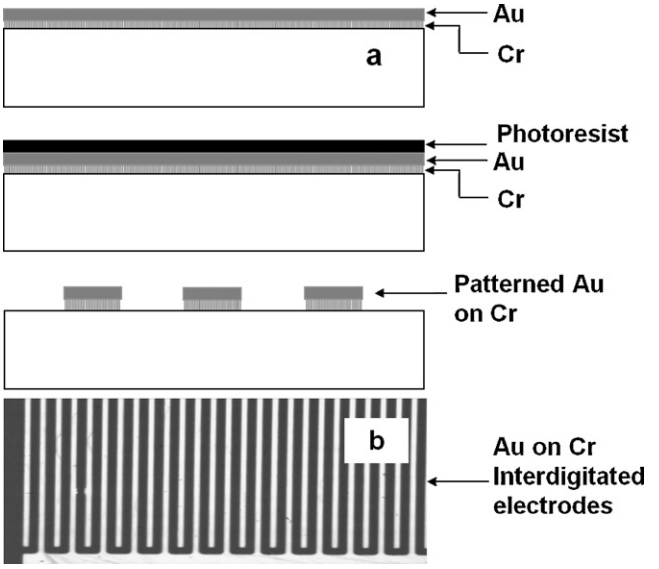

Fig. 1. (a) Fabrication process flow of IME array. A thin Cr/Au film is deposited on top of a glass substrate. The film is patterned into individual conductive traces using contact photolithography and etching processes. (b) optical images of the interdigitated microelectrode (IME).

adhesion promoter. The interdigitated electrodes were fabricated by etching the patterned Au on Cr, as shown in Fig. 1.

2.2. Culture preparation of bacteria

2.2.1. E. coli broth preparation

For the *E. coli* broth preparation, 33 g of the mTSB (modified Tryptone Soya Broth) with novobiocin (Sigma–Aldrich, St. Louis, MO) was suspended into 1000 ml of distilled water. The solution was heated to 120 °C using the Isotemp hot plate (Fisher Scientific) for 15 min. *E. coli* grown on a previously cultured plate was obtained using an inoculating loop (Fisher Scientific) and the broth was inoculated with the *E. coli*. The contaminated broth was incubated for about 24 h before it was used. The *E. coli* was obtained from a lab at the University of Missouri-Columbia. The *E. coli* was cultured over a period of time in our lab, using Macconkey Sorbitol Agar (Remel Inc., Lenexa, KS).

2.2.2. Agar preparation

To make agar, 1000 ml of distilled water was boiled and 50 g of Macconkey Sorbitol Agar was added to it. The solution was brought to a boil and left to boil for 7–10 min. It was then removed from the hot plate and left to cool. Once cooled, the agar mixture was poured onto the sterilized Petri dishes (Fisher Scientific) and labeled.

2.2.3. Antibody preparation

The goat anti *E. coli* 0157:H7 antibody was obtained from (Biodesign International, Saco, ME). The antibody was diluted to a concentration of 50 μg ml^{-1} in PBS solution (Boston Bio-products, Boston, MA).

2.2.4. E. coli preparation

Contaminated broth measuring 3 ml was centrifuged (Horizon 642VES, Drucker Company, PA) at 3200 rpm for 10 min. After the centrifugation, the supernatant was removed and the cells were re-dispersed in 3 ml PBS (Phosphate Buffer Saline). The re-dispersed cells were centrifuged at 3200 rpm for 10 min and the step was repeated. The concentration of final purified cell suspension was approximately 2.5×10^6 CFU ml^{-1}. After the centrifugation was complete, the supernatant was removed and the cells were re-dispersed in 500 μl PBS solution.

2.3. Antibody immobilization

Goat anti-*E. coli* IgG antibodies (Biodesign International, Saco, ME) were diluted to a concentration of 50 μg ml^{-1} in PBS solution (Boston Bio-products, Boston, MA). This antibody concentration was determined as the lowest concentration that produced a maximum impedance change, and showed the highest surface coverage, minimizing any subsequent nonspecific adsorption. The antibodies were immobilized to the gold electrode surface as shown in Fig. 2. The PDMS slab with a rectangular hole cut in it was bonded to the fabricated IME device. This well like PDMS structure holds the media containing antibody over the IME. A volume of 100 μl antibody solution was pipetted into the PDMS reservoir. The media was left on the IDEA for 2 h, during which the antibody was allowed to adsorb non-specifically to the gold electrode surface. After 2 h, the media was pipetted out, and any unbounded antibodies were washed carefully using DI water. In the next step, 100 μl of *E. coli* was pipetted over the immobilized antibodies. *E. coli* was bound to the antibody. Any unbounded *E. coli* was washed away using DI water, leaving the securely bonded antigen/antibody on the IDEA.

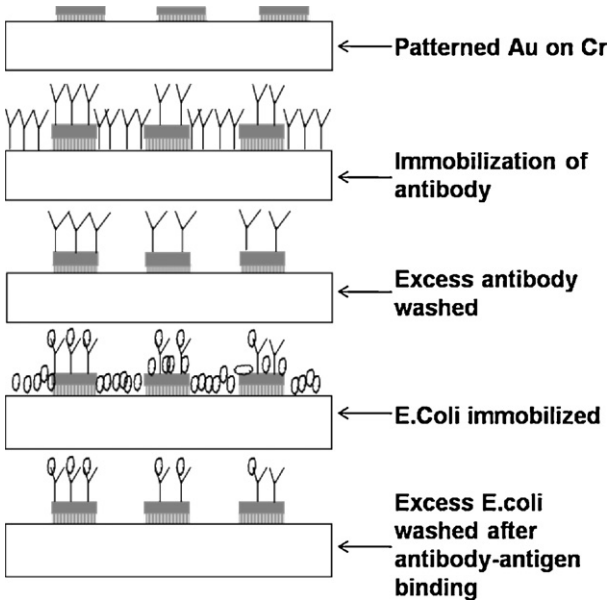

Fig. 2. Process-flow of the immobilization of antibody, and the antibody/antigen binding on the interdigitated microelectrode (IDEA).

2.4. Sensor response range

Dose response and time response studies were performed as part of this study. The dose response study included concentrations of 0 CFU ml^{-1}, 2.5×10^4 CFU ml^{-1}, 2.5×10^5 CFU ml^{-1}, 2.5×10^6 CFU ml^{-1} and 2.5×10^7 CFU ml^{-1}. The time response study included immobilizing the *E. coli* for 30 min, 60 min and 120 min, while keeping the concentration of 2.5×10^6 CFU ml^{-1} constant. This choice of concentration was made because, from the dose response studies, it was inferred that this concentration might be optimal.

2.5. Data acquisition

The impedance measurement was performed using Agilent 4294A impedance analyzer. The set-up used for data acquisition is shown in Fig. 3. A sine wave of 500 mV peak voltage was applied across the terminals of the IDEA arrays and the corresponding impedance values were measured for frequencies between 100 Hz and 10 MHz. The impedance values for the dose were calculated

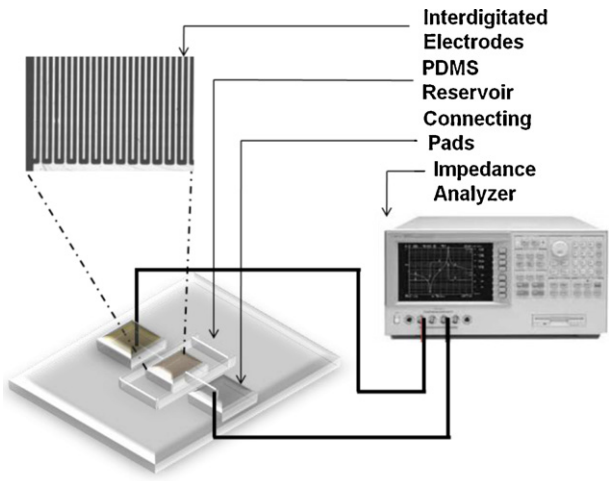

Fig. 3. Schematic of the test set-up for measuring impedance.

in terms of percentages. This was performed because the raw impedance values for different devices had different starting points, and only changed a few percent after exposure to the antigen. Hence if only the difference of antibody (Ab) and antibodies (Ag) value were to be taken into account, it would be difficult to see a significant change in the impedance values. This is why using percentages is beneficial and more accurately reflects the change that has taken place.

2.6. Protocol for device reusability

After each measurement, the microelectrode array was cleaned using organic and plasma cleaning. The device was reused, following a cleaning protocol that included treating the device in acetone for 30 min, followed by a wash with isopropanol and DI water. This is followed by an exposure to plasma for 2 min with a power of 48 W. This cleaning protocol was used successfully for at least 20 devices over the course of the study, and the devices were reused 5 times each.

3. Results and discussion

3.1. Fluorescence imaging of immobilized E. coli

A suspension of *E. coli* was immersed in a hot water bath at 80 °C for 1 h to kill the bacteria. The resulting cell suspension was labeled with FITC. A clean unused IDEA device was activated by adsorption of anti-*E. coli* antibody. The antibody, at a concentration of 50 μl ml^{-1}, was exposed to electrode for 1 h. The electrode was then rinsed with distilled water to remove any unbounded antibody. The device was then exposed to the labeled cells at a concentration of 2.5×10^6 CFU ml^{-1} for 1 h, and was then rinsed again with distilled water to remove unbound *E. coli*. A volume of 10 μl distilled water was pipetted onto the surface of the device, and it was covered with a plastic cover slip. For comparison, and to ensure effective fluorescent labeling of the cells, a 10 μl volume of labeled cell suspension was pipetted onto a microscope slide and covered with a plastic cover slip.

The cell suspension on a glass microscope slide with labeled rod-shaped bacteria is shown in Fig. 4a. It is worth noting that after purification; vortexing the labeled cell suspension was ineffective at breaking up and distributing the cells completely evenly, as shown by the large clumps of cells visible in the image. The image in Fig. 4b, shows labeled cells bound to the IDEA device. Although many cells are bound to the gold (light gray lines in the image), a number of cells were adsorbed onto the glass voids between electrodes (dark gray sections in the image). It was anticipated that the higher affinity of the *E. coli* to the specific antibodies would cause preferential binding of the cells to the antibody-covered electrodes. The results, however, show that binding is occurring on both surfaces. In order to ensure adsorption onto only the microelectrode, it is proposed for future similar studies, to chemically modify the surface to keep non-specific cell types from binding to the glass voids between electrodes.

3.2. The equivalent circuit of the IDEA impedance sensor

The equivalent circuit of the IDEA impedance device in a solution is represented by the circuit shown in Fig. 5a [41,42]. The components of this circuit include two capacitors (C_{dl}) representing the double layer capacitances of the IDEA's and (R_{sol}) representing the solution resistance connected in series. The (C_{di}) which is connected in parallel represents the dielectric capacitance. When an alternating potential is applied to the device, the impedance (Z)

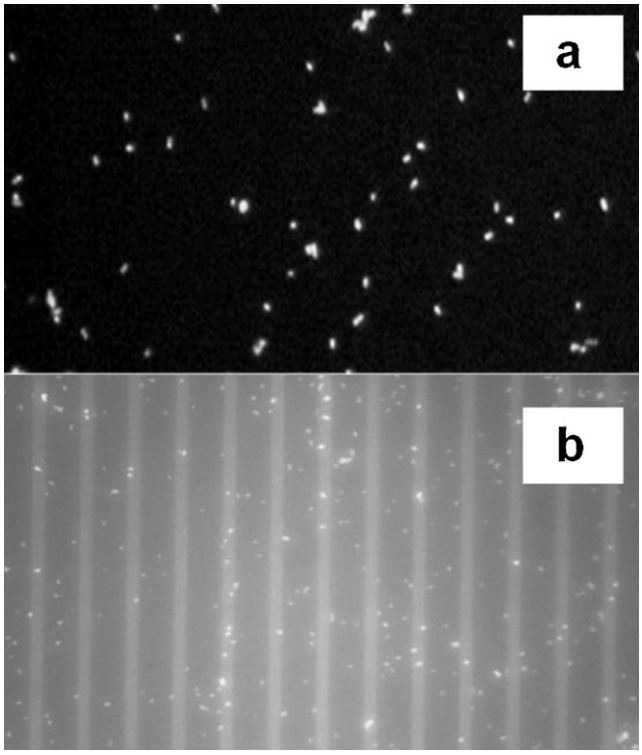

Fig. 4. Fluorescence Image of (a) an image of the cell suspension only on a glass microscope slide. This image clearly shows the labeled rod-shaped bacteria. It is worth noting that after purification; vortexing the labeled cell suspension was ineffective at breaking up and distributing the cells, as shown by the large clumps of cells visible in the image. (b) An image of the labeled cells bound to the IDEA device. This image shows a large number of cells bound to the device.

is a function of the capacitance and the resistances, and is denoted as:

$$|Z_1| = \sqrt{R_{sol}^2 + \frac{1}{(\pi f C_{dl})^2}}$$

This equation represents the impedance due to (C_{dl}) and (R_{sol}) which are dominant at low frequencies, with (C_{dl}) being dominant till between 40 Hz and 300 Hz as shown in the impedance spectrum in Fig. 5b. The second region between 300 Hz and 10 KHz is a combination of (C_{dl}) and (R_{sol}). Dielectric capacitance (C_{di}) is represented by the equation:

$$|Z_2| = \sqrt{\frac{1}{(2\pi f C_{di})^2}} \quad (2)$$

The third region is in frequency ranges above 1 MHz, and the signal in this region is dominated by the dielectric behavior of the medium.

Therefore, the total resistance of the system is given by:

$$\frac{1}{Z_{tot}} = \frac{1}{Z_1} + \frac{1}{Z_2} \quad (3)$$

The experimental and curve fitted data based on the equivalent circuit for impedance measurement of sample concentration of 2.5×10^6 CFU ml^{-1} of *E. coli O157:H7* are shown in Fig. 5b. Software from EIS analyzer was used for simulation and fitting of the data. For data validation, 50 points were chosen by the software and used in generating a fitting impedance spectrum.

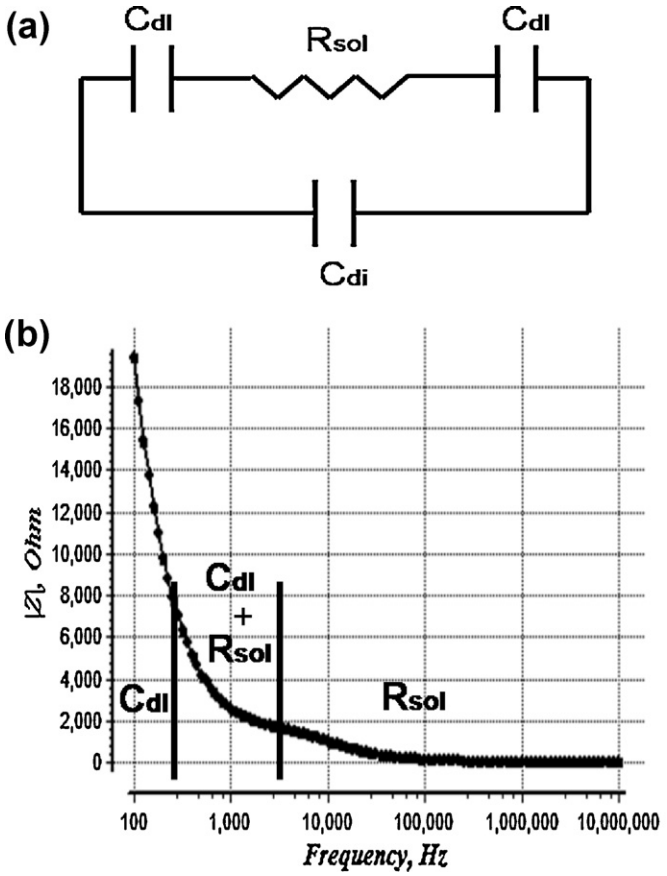

Fig. 5. (a) The equivalent circuit of the impedance measurement system with interdigitated electrode. (b) An impedance spectrum together with the fitting curve. C_{dl} is the double layer capacitance at each electrode; R_{sol} is the resistance of the medium; C_{di} is the dielectric capacitance of medium.

3.3. Detection of E. coli using impedance sensing

The Interdigitated Microelectrode (IDEA) array has high sensitivity toward impedance change. It is observed that the impedance changes as antibody is immobilized on the IDEA, as compared with just the control solution on the bare electrode surface. Likewise there is a change in value of impedance when the *E. coli* binds to the antibody. Bacterial cells, when present in between two electrical conductors can conduct, creating a lower resistive path between the two conductors. Cell wall, cytoplasm and few other cell components act as conductors. Detection of bacterial cells based on measurement of impedance can be analyzed using the relationship between impedance and frequency. The detection range of the device is plotted in Fig. 6. The operating range of the device is between 2.5×10^4 CFU ml^{-1} to 2.5×10^7 CFU ml^{-1}. Concentrations of *E. coli* above 2.5×10^7 CFU ml^{-1} were extremely turbid and concentrated, and hence not tested. The graph between the frequency and the magnitude for different concentrations is shown in Fig. 7a. For all concentrations the impedance values decrease as a function of frequency. The magnitude of impedance is lower for smaller concentrations, and increases with increase in concentration. The phase is also a function of frequency, and decreases with increase in frequency for the respective concentrations as shown in Fig. 7b.

To test the effect of time on antigen/antibody binding, a constant concentration (2.5×10^6 CFU ml^{-1}) of antigen was used but the binding times were changed. The times used were 30 min, 60 min and 120 min. The time response is plotted in Fig. 8. This study was performed to see the minimal optimum time needed for the antibody/antigen binding to detect an appreciable change in impedance values to confirm the presence of *E-coli* in the sample. Allowing the binding to take place for extended periods of time beyond the optimum time required for antigen/antibody binding might have a negative effect on the experimental values. Extended amount of binding time does not provide any additional advantage, but only adds to the time. It should be noted that the value of impedance for 60 min time response is higher than the value for 120 min time response. It is possible that after 60 min, the bacteria are slowing the process of release that is causing the impedance decrease.

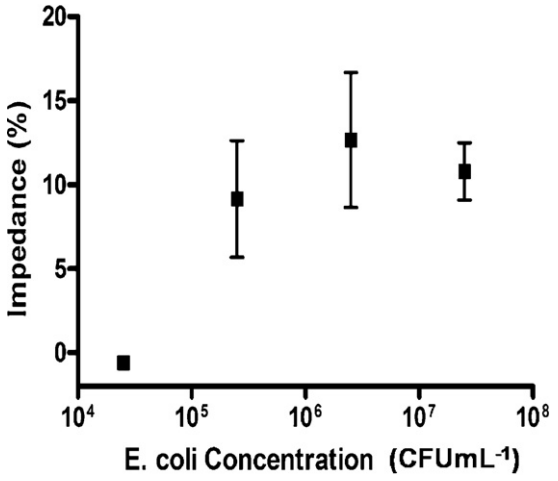

Fig. 6. Graph showing the relation between the concentrations of the *E. coli* vs. impedance (%) (dose response).

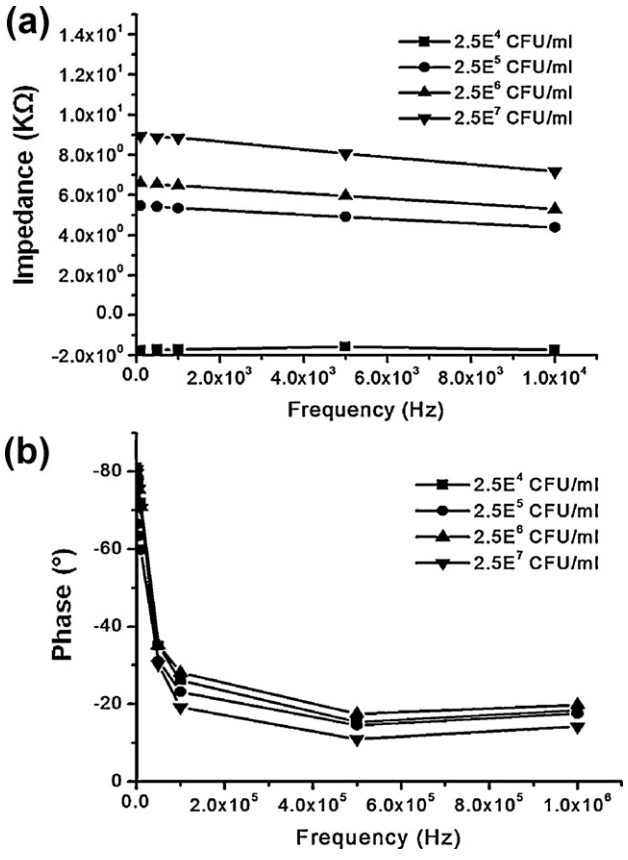

Fig. 7. (a) Graph between the frequencies vs. impedance. The value of impedance measured decreases as a function of increasing frequency. (b) Graph between the frequencies vs. phase.

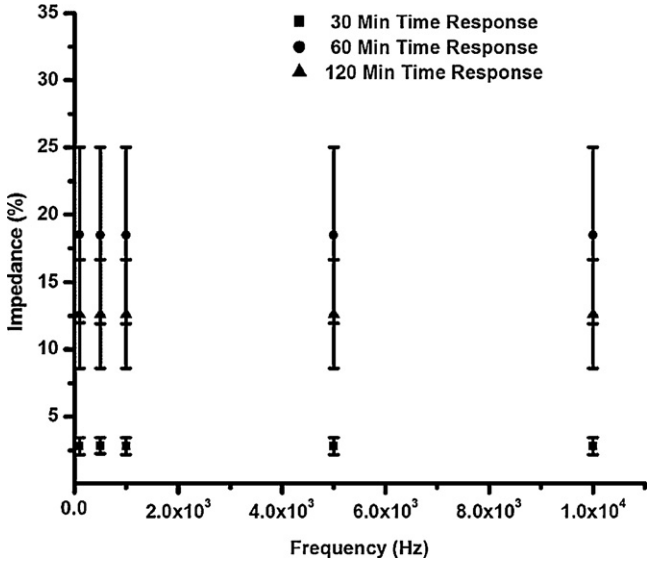

Fig. 8. Graph showing the relation between the concentrations of the *E. coli* vs. impedance (%) (time response).

4. Conclusion

A simple, sensitive and reusable impedance sensing platform for the detection of viable *E. coli O157:H7* was fabricated. The sensor was able to detect the bacteria, both qualitatively and quantitatively. The advantage of this sensor over other similar sensors is the specific and targeted detection of the bacteria with a sensitive working range. The other advantages of this device are the faster results and reusability. This platform can also be used for detection of other bacteria by immobilizing the antigen specific antibody.

Acknowledgments

This project is supported in part by USDA-Evans Allen Fund and National Science Foundation Grant No. ECCS-0925612.

References

[1] http://www.cdc.gov/mmwr/preview/mmwrhtml/mm6022a5.htm?s_cid=mm6022a5_w.
[2] http://www.cdc.gov/nczved/divisions/dfbmd/diseases/ecoli_o157h7/#spread.
[3] http://www.cdc.gov/ecoli/index.htm#selectpubs.
[4] W.M. Fedio, K.C. Jinneman, K.J. Yoshitomi, R. Zapata, C.N. Wendakoon, P. Browning, S.D. Weagant, International Journal of Food Microbiology 148 (2011) 87–92.
[5] N.Y. Fortin, A. Mulchandani, W. Chen, Analytical Biochemistry 289 (2001) 281–288.
[6] Y. Liu, Y. Li, Journal of Microbiological Methods 51 (2002) 369–377.
[7] A. Subramanian, J. Irudayaraj, T. Ryan, Biosensors & Bioelectronics 21 (2006) 998–1006.
[8] J. Waswa, J. Irudayaraj, C. DebRoy, LWT 40 (2007) 187–192.
[9] L. Wang, Q. Liu, Z. Hu, Y. Zhang, C. Wu, M. Yang, P. Wang, Talanta 78 (2009) 647–652.
[10] E.B. Setterington, E.C. Alocilja, Biosensors & Bioelectronics 26 (2011) 2208–2214.
[11] D. Li, Y. Feng, L. Zhou, Z. Ye, J. Wang, Y. Ying, C. Ruan, R. Wang, Y. Li, Analytica Chimica Acta 687 (2011) 89–96.
[12] S.-H. Huang, Sensors and Actuators B 133 (2008) 561–564.
[13] J.C. Pyun, H. Beutel, J.-U. Meyer, H.H. Ruf, Biosensors & Bioelectronics 13 (1998) 839–845.
[14] J.J. Varela-Hernández, E. Cabrera-Diaz, M.A. Cardona-López, L.M. Ibarra-Velázquez, H. Rangel-Villalobos, A. Castillo, M.R. Torres-Vitela, A. Ramírez-Álvarez, International Journal of Food Microbiology 113 (2007) 237–241.
[15] H. Tang, W. Zhang, P. Geng, Q. Wang, L. Jin, Z. Wu, M. Lou, Analytica Chimica Acta 562 (2006) 190–196.
[16] Y.-H. Lin, S.-H. Chen, Y.-C. Chuang, Y.-C. Lua, Y. Thomas, C. Shen, Allen Chang, Chih-Sheng Lin, Biosensors & Bioelectronics 23 (2008) 1832–1837.
[17] J.-J. Gau, E.H. Lan, B. Dunn, C.-M. Ho, J.C.S. Woo, Biosensors & Bioelectronics 16 (2001) 745–755.
[18] M.M. Werneck, R.M. Ribeiro, Biosensors & Bioelectronics 16 (2001) 399–408.
[19] K. Rijal, A. Leung, P.M. Shankar, R. Mutharasan, Biosensors & Bioelectronics 21 (2005) 871–880.
[20] L. Yang, R. Bashir, Biotechnology Advances 26 (2008) 135–150.
[21] H. Shiraishi, T. Itoh, H. Hayashi, K. Takagi, M. Sakane, T. Mori, J. Wang, Bioelectrochemistry 70 (2007) 481–487.
[22] Q. Yang, Y. Liang, T. Zhou, G. Shi, L. Jin, Electrochemistry Communications 11 (2009) 893–896.
[23] Z.-Q. Shen, J.-F. Wang, Z.-G. Qiu, M. Jin, X.-W. Wang, Z.-L. Chen, J.-W. Li, F.-H. Cao, Biosensors & Bioelectronics 26 (2011) 3376–3381.
[24] V. Escamilla-Gomez, S. Campuzano, M. Pedrero, J.M. Pingarron, Biosensors & Bioelectronics 24 (2009) 3365–3371.
[25] M. Uyttendaele, S. van Boxstael, J. Debevere, International Journal of Food Microbiology 52 (1999) 85–95.
[26] T. Bryan Tims, D.V. Lim, Journal of Microbiological Methods 55 (2003) 141–147.
[27] Z. Fu, S. Rogelj, T.L. Kieft, International Journal of Food Microbiology 99 (2005) 47–57.
[28] S.D. Weagant, K.C. Jinneman, K.J. Yoshitomi, R. Zapata, W.M. Fedio, International Journal of Food Microbiology (2011).
[29] R.E. Brackett, J.F. Frank, K.H. Seo, International Journal of Food Microbiology 44 (1998) 115–123.
[30] M. Varshney, Y. Li, B. Srinivasan, S. Tung, Sensors and Actuators B 128 (1) (2007) 99–107.
[31] A.D. Taylor, Q. Yu, S. Chen, J. Homola, S. Jiang, Sensors and Actuators B 107 (2005) 202–208.
[32] E. Baldrich, F. Javier del Campo, F. Xavier Muñoz, Biosensors & Bioelectronics 25 (2009) 920–926.
[33] I. Burdallo, C. Jiménez-Jorquera, Procedia Chemistry 1 (2009) 289–292.
[34] M. Barreiros dos Santos, C. Sporer, N. Sanvicens, N. Pascual, A. Errachid, E. Martinez, M.-P. Marco, V. Teixeira, J. Samiter, Procedia Chemistry 1 (2009) 1291–1294.
[35] M.B. Mejri, H. Baccar, E. Baldrich, F.J. Del Campo, S. Helali, T. Ktari, A. Simonian, M. Aounid, A. Abdelghani, Biosensors & Bioelectronics 26 (2010) 1261–1267.
[36] S. Bayoudh, A. Othmane, L. Ponsonnet, H. Ben Ouada, Colloids and Surfaces A: Physicochemical and Engineering Aspects 318 (2008) 291–300.
[37] M. Varshney, Y. Li, Talanta 74 (2008) 518–525.
[38] L. Yang, Talanta 74 (2008) 1621–1629.
[39] S. Barizuddin, X. Liu, J.C. Mathai, M. Hossain, K.D. Gillis, S. Gangopadhyay, ACS Chemical Neuroscience 1 (2010) 590–597.
[40] X. Liu, S. Barizuddin, W. Shin, C.J. Mathai, S. Gangopadhyay, K.D. Gillis, Analytical Chemistry 83 (7) (2011) 2445–2451.
[41] P. Van Gerwen, W. Laureyn, W. Laureys, G. Huyberechts, M. Op De Beeck, K. Baert, J. Suls, W. Sansen, P. Jacobs, L. Hermans, R. Mertens, Sensors and Actuators B 49 (1998) 73–80.
[42] L. Yang, Y. Li, C.L. Griffs, M.G. Johnson, Biosensors & Bioelectronics 19 (2004) 1139–1147.